THE JOURNAL OF BIOLOGICAL CHEMISTRY Vol. 272, No. 43, Issue of October 24, pp. 27160–27166, 1997
Printed in U.S.A.

Functional Domain Mapping of the Clathrin-associated Adaptor Medium Chains μ1 and μ2*

(Received for publication, July 7, 1997, and in revised form, August 8, 1997)

Ruben C. Aguilar, Hiroshi Ohno, Katherine W. Roche, and Juan S. Bonifacino‡

From the Cell Biology and Metabolism Branch, NICHD, National Institutes of Health, Bethesda, Maryland 20892-5430

The clathrin-associated adaptors AP-1 and AP-2 are heterotetrameric complexes involved in the recognition of sorting signals present within the cytosolic domain of integral membrane proteins. The medium chains of these complexes, μ1 and μ2, have been implicated in two types of interaction: assembly with the β1 and β2 chains of the corresponding complexes and recognition of tyrosine-based sorting signals. In this study, we report the results of a structure-function analysis of the μ1 and μ2 chains aimed at identifying regions of the molecules that are responsible for each of the two interactions. Analyses using the yeast two-hybrid system and proteolytic digestion experiments suggest that μ1 and μ2 have a bipartite structure, with the amino-terminal one-third (residues 1–145 of μ1 and μ2) being involved in assembly with the β chains and the carboxyl-terminal two-thirds (residues 147–423 of μ1 and 164–435 of μ2) binding tyrosine-based sorting signals. These observations support a model in which the amino-terminal one-third of μ2 is embedded within the core of the AP-2 complex, while the carboxyl-terminal two-thirds of the protein are exposed to the medium, placing this region in a position to interact with tyrosine-based sorting signals.

The clathrin-associated adaptors AP-1 and AP-2 are heterotetrameric complexes that mediate attachment of clathrin to membranes and recruitment of integral membrane proteins for incorporation into clathrin-coated vesicles (reviewed in Refs. 1 and 2). AP-1 is localized to the *trans*-Golgi network, where it mediates biosynthetic protein transport to the endosomal/lysosomal system, whereas AP-2 is localized to the plasma membrane and mediates rapid internalization of endocytic receptors. AP-1 is composed of four chains termed γ (~91 kDa), β1 (~101 kDa), μ1 (~47 kDa), and σ1 (~19 kDa). The four chains of AP-2 are homologous to those of AP-1 and are known as α (~104–108 kDa), β2 (~104 kDa), μ2 (~50 kDa), and σ2 (~17 kDa), respectively. The homologous chains of each complex are thought to subserve similar structural and functional roles. Two of the "large" chains, γ and α, mediate specific targeting of the corresponding adaptors to the *trans*-Golgi network and the plasma membrane, respectively (3, 4). The other large chains, β1 and β2, have been implicated in clathrin binding (5–8). A role for the α chain in clathrin binding has also been proposed (9). Recent work has demonstrated that μ1 and μ2 (known as the "medium" chains) bind tyrosine-based sorting signals present within the cytosolic domain of some integral membrane proteins and thus probably mediate the capture of these proteins into clathrin-coated areas of the membranes (10–14). The function of the σ1 and σ2 chains (referred to as the "small" chains) is currently unknown.

The overall structure of the adaptor complexes and the arrangement of the different chains within them have been studied using various approaches. Analyses by deep-etch electron microscopy have revealed that the AP-2 complex has a brick-shaped core of ~8 nm ("head") with two smaller appendages of ~2–3 nm ("ears") separated from the core by thin linker strands ("hinges") (15). Mild proteolysis of AP-2 resulted in the release of both ears, leaving a head composed of ~60–65-kDa amino-terminal fragments of α and β2, and intact μ2 and σ2 (6, 16–18). The division of the adaptor large chains into head, hinge, and ear domains suggested by the combination of electron microscopy and limited proteolysis analyses was further supported by sequence comparisons with structural homologs of α (*i.e.* γ (19) and δ (20, 21)) and β2 (*i.e.* β1 (18, 22), β3A (23, 21), and β3B (originally referred to as β-NAP, Ref. 24)), which revealed three distinct regions with different degrees of sequence conservation. Although the AP-1 complex has not yet been visualized by electron microscopy, limited proteolysis and sequence analyses of its chains suggest that it has an overall structure similar to AP-2 (6, 19).

Additional insight into the structure of the AP-1 and AP-2 complexes was obtained from analyses of subunit interactions using the yeast two-hybrid system (4). This approach revealed the following pairwise interactions for AP-1 subunits: γ-β1, γ-σ1, and β1-μ1; the analogous interactions observed for AP-2 were α-β2, α-σ2, and β2-μ2. Interactions were also detected between the β and μ chains of different AP complexes (*i.e.* β1-μ2 and β2-μ1), which suggests that β1 and β2 may be interchangeable within the complexes. This is not surprising, since β1 and β2 are very closely related (85% identity and 92% similarity; Refs. 18, 22, and 25). As expected from previous structural studies, all interactions involving the large chains (γ, α, β1, and β2) occurred at the level of their head domains (4).

In contrast to the detailed information that is now available about the structure of the large chains, very little is known about the domain organization of the μ chains, as well as their arrangement within the AP complexes. These chains have been implicated in two types of interaction: assembly with the β chains (4) and recognition of tyrosine-based sorting signals (10–12). The regions of the molecules that are responsible for these functions and the relationship of these regions to the rest of the complex have not been established. In this study, we present a structure-function analysis of the μ chains aimed at identifying the domains that interact with the β chains and with tyrosine-based sorting signals. These analyses reveal that both μ1 and μ2 can be functionally dissected into two parts: an amino-terminal one-third (residues 1–145 of μ1 and μ2) that

* The costs of publication of this article were defrayed in part by the payment of page charges. This article must therefore be hereby marked "*advertisement*" in accordance with 18 U.S.C. Section 1734 solely to indicate this fact.

‡ To whom correspondence should be addressed: CBMB, NICHD, National Institutes of Health, Bldg. 18T, Rm. 101, 18 Library Dr. MSC 5430, Bethesda, MD 20892-5430. Tel.: 301-496-6368; Fax: 301-402-0078; E-mail: juan@helix.nih.gov.

interacts with the β chains and the carboxyl-terminal two-thirds (residues 147–423 of μ1 and 164–435 of μ2) that bind tyrosine-based sorting signals. These observations suggest a model in which the amino-terminal one-third of μ2 is embedded within the AP-2 head via interaction with β2, whereas the carboxyl-terminal two-thirds of the protein project outward from the head, placing this domain in a position to interact with tyrosine-based sorting signals.

EXPERIMENTAL PROCEDURES

Recombinant DNA Constructs—The constructs GAL4 DNA-binding domain (GAL4bd)[1]-TGN38 Tail Δ1 (YQRL), GAL4bd-TGN38 Tail Δ1 (AQRL), GAL4ad-μ1, and GAL4ad-μ2 have been described previously (10, 11). The construct GAL4bd-β2 was kindly provided by Dr. M. S. Robinson (Department of Clinical Biochemistry, University of Cambridge, Cambridge, United Kingdom). All of the other two-hybrid constructs were made by ligation of polymerase chain reaction products into the pGBT9 or pACTII vectors (CLONTECH, Palo Alto, CA). The nucleotide sequences of all the recombinant constructs were confirmed by dideoxy sequencing.

Yeast Culture, Transformation, and Two-hybrid Assays—The *Saccharomyces cerevisiae* strain HF7c (*MATa, ura3–52, HIS3-200, lys 2–801, ade2–101, trp1–901, leu2–3, 112, gal4–542, gal80–538, LYS2::GAL1-HIS3*, *URA3::(GAL4* 17-mers)$_3$-*CYC1-lacZ*) (CLONTECH) was maintained on YPD agar plates. Transformation was done by the lithium acetate procedure as described in the instructions for the MATCHMAKER two-hybrid kit (CLONTECH). For colony growth assays, HF7c transformants were streaked on plates lacking leucine, tryptophan, and histidine and allowed to grow at 30 °C, usually for 4–5 days, until colonies were large enough for further assays. Quantitative growth assays were carried out as follows; 3–5 colonies of each HF7c transformant were added to 20 ml of liquid medium lacking histidine (−His medium) and grown at 30 °C to 1.0–1.2 OD_{600}/ml. Cultures (3×10^{-3} OD_{600} units, ~3 μl) were then inoculated into 20 ml of −His medium in the absence or presence of several concentrations of 3AT (3-amino-1,2,4-triazole, Fluka Chemie AG, Buchs, Switzerland). After 2 days of incubation at 30 °C, the OD_{600} of triplicates were measured. Results were expressed as the ratio of the signal obtained in the presence of 3AT and the signal obtained in its absence (control). β-Galactosidase assays of HF7c transformants in liquid culture (5–7 colonies/culture) were done using a chemiluminescent β-galactosidase assay kit (CLONTECH). Briefly, yeast cells were resuspended at 10 OD_{600}/ml in lysis buffer (100 mM sodium phosphate, 1 mM dithiothreitol, pH 7.4) and broken by vortexing in the presence of glass beads. After centrifugation at 4 °C for 15 min in a microcentrifuge, 10–50 μl of the lysate was added onto 200 μl of kit reaction buffer, incubated for 1 h at room temperature, and the light emission recorded as a 5-s integral in a tube luminometer (Monolight 2010, Analytical Luminescence Laboratory, San Diego, CA). Results were normalized by protein concentration and expressed as the mean ± standard deviation of three independent determinations.

Site-directed Mutagenesis—Single amino acid substitutions to alanine in μ2 were made using the QuickChange site-directed mutagenesis kit (Stratagene, La Jolla, CA). Briefly, 50 ng of pGBT9 or pACTII plasmids carrying the μ2 chain cDNA were incubated with two complementary primers (2 μM each) containing the desired mutation in the presence of 2 mM dNTP mix and 2.5 units of *Pfu* DNA polymerase for 16 cycles according to the following temperature profile: 0.5 min at 95 °C, 1 min at 55 °C, and 8 or 16 min at 68 °C. After replication of both vector strands, the methylated parental DNA was digested for 1 h at 37 °C with 10 units of *Dpn*I endonuclease, and the nicked vector having the desired mutation was transformed into *Escherichia coli*.

Trypsin Digestion of Clathrin-coated Vesicles and Immunoblotting—Proteolytic cleavage of adaptor complexes was performed by incubating clathrin-coated vesicles (total protein concentration: 500 μg/ml; vesicles were kind gifts of E. Eisenberg and L. Green, NHLBI, National Institutes of Health and T. Kirchhausen, Harvard Medical School, Boston, MA) with different concentrations (1–1250 μg/ml) of trypsin (Sigma) for 10 min at 37 °C in phosphate-buffered saline, 5 mM $MgCl_2$, 1 mM dithiothreitol, pH 7.4. The reaction was stopped by addition of 50 mM soybean trypsin inhibitor (Sigma), and the digested samples were analyzed by SDS-PAGE (4–20% precast gradient gels; Novex, San Diego, CA) and electroblotted onto nitrocellulose. After incubation with primary antibodies to AP-2 chains and horseradish peroxidase-conjugated secondary antibodies, bands were detected using the ECL system (Amersham).

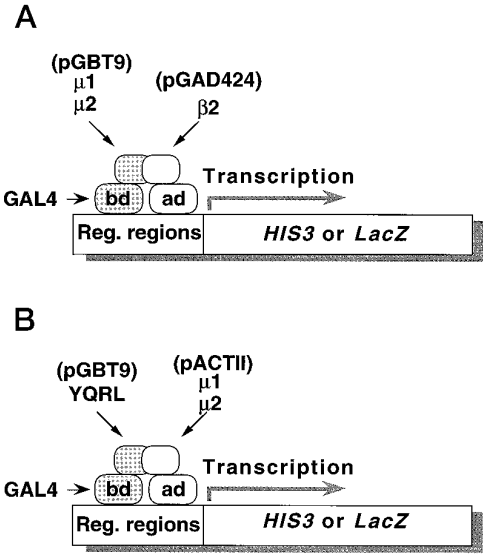

FIG. 1. **Schematic representation of the two-hybrid analyses performed in this study.** Interactions of μ chains with β2 (*A*) or with the YQRL signal (*B*) were analyzed by the two-hybrid system of Fields and Song (31). *A*, GAL4bd-μ1 or GAL4bd-μ2 constructs in pGBT9 (TRP1) were co-expressed with a GAL4ad-β2 construct in pGAD424 (LEU2). *B*, GAL4ad-μ1 or GAL4ad-μ2 in pACTII (LEU2) were co-expressed with GAL4bd-YQRL in pGBT9 (TRP1). Yeast strains co-expressing GAL4bd and GAL4ad constructs were selected in media lacking leucine and tryptophan. Interactions between the GAL4bd and GAL4ad fusion proteins result in transcription of the *HIS3* and *lacZ* reporter genes, which are detected by growth of the yeast cells in media lacking histidine and by expression of β-galactosidase activity, respectively. *Reg. regions*, regulatory regions containing upstream activation and promoter sequences.

Antibodies—A rabbit polyclonal antiserum (R11–29) to an amino-terminal sequence of the μ2 chain was obtained by immunization with a peptide corresponding to residues 11–29 of mouse μ2 (KGEVLIS-RVYRDDIGRNAV). This antibody was specific for μ2 and did not recognize the related protein μ1 (data not shown). Other antibodies used were: AC1-M11 (anti-α, Ref. 26, kindly provided by M. S. Robinson, Department of Clinical Biochemistry, University of Cambridge, Cambridge, UK), 100/2 (anti-α, Ref. 27, obtained from Sigma), 100/1 (anti-β, Ref. 27, obtained from Sigma), and C420-A9 (anti-β, kindly provided by T. Kirchhausen).

Sequence Analysis—Sequences from different μ chains were compared using the PLOTSIMILARITY program from the Wisconsin Package (version 8.1-UNIX, Genetics Computer Group, Madison, WI), and μ2 loop probability was calculated using the neural network prediction system PHD (28–30).

RESULTS

Interactions of μ1 and μ2 with β2 and with a Tyrosine-based Sorting Signal—Previous studies have demonstrated that the clathrin-associated adaptor medium chains μ1 and μ2 interact with the β2 chain of AP-2 (4) and with Y*XX*Ø-type[2] tyrosine-based sorting signals (10–12). To further characterize these interactions, we used a yeast two-hybrid system in which the interacting polypeptides were expressed as fusions with the activation or binding domains of the transcriptional activator GAL4 (31) (Fig. 1). Association of the two GAL4 domains driven by interacting polypeptides leads to activation of transcription of the *HIS3* gene, which allows growth in defined media lacking histidine (−His), and of the *lacZ* gene, which results in expres-

[1] The abbreviations used are: GAL4bd, GAL4 DNA-binding domain; GAL4ad, GAL4 transcription activation domain; 3AT, 3-amino-1,2,4-triazole; PAGE, polyacrylamide gel electrophoresis; CCV, clathrin-coated vesicle.

[2] Y is tyrosine, *X* is any amino acid, and Ø is an amino acid with a bulky hydrophobic side chain (leucine, isoleucine, phenylalanine, methionine, or valine).

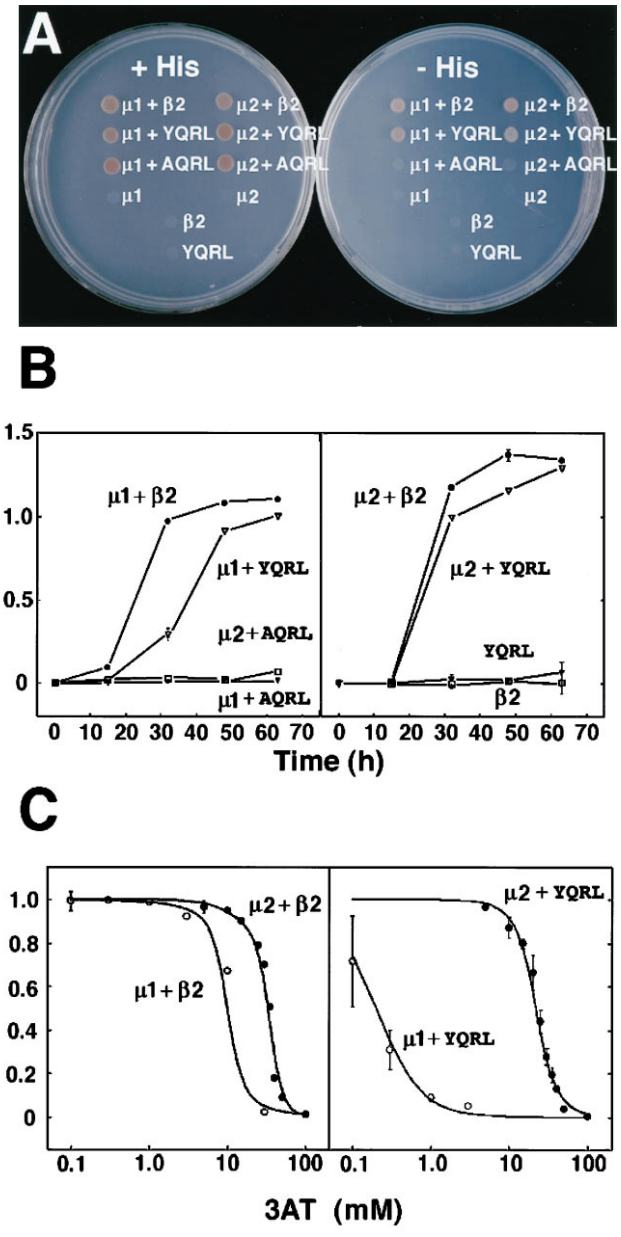

FIG. 2. **Both μ1 and μ2 interact with β2 and with the tyrosine-based signal YQRL.** *A*, plate growth assay. Yeast transformants expressing the constructs indicated in the figure were spotted onto plates lacking leucine and tryptophan, with or without histidine (+*His* and −*His*, respectively). Only those transformants expressing interacting constructs were able to grow in the absence of histidine. Transformants expressing only μ1, μ2, β2, or the YQRL signal were included in the assay as negative controls. *B*, growth assay in liquid culture. Yeast transformants expressing different combinations of constructs were cultured in −His liquid medium, and the optical density at 600 nm (OD_{600}) was measured at different times. The growth rate in this assay depends on the expression levels of the *HIS3* product. Transformants expressing only β2 or the YQRL signal were included as negative controls. *C*, 3AT growth inhibition assay. The interactions indicated in the figure were characterized by analyzing the effect of increasing concentrations of the histidine biosynthesis inhibitor 3AT on the growth of co-transformed yeast cells. Values on the *y* axis are the ratios of OD_{600} in the presence or absence of 3AT. Values are the mean ± S.D. of triplicate determinations.

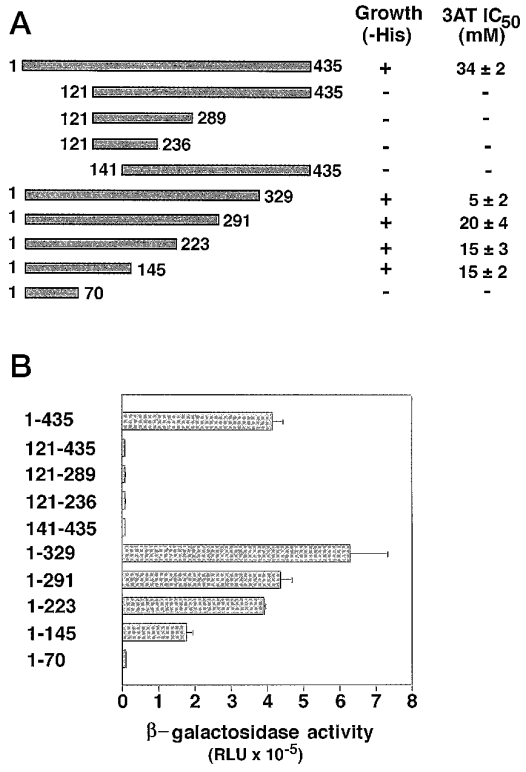

FIG. 3. **Analysis of the interaction of β2 with μ2 deletion mutants.** Interactions were analyzed by transformation of yeast cells with plasmids encoding GAL4ad-β2 and GAL4bd-μ2 deletion mutants (as shown in Fig. 1*A*). *A*, diagram of the μ2 deletion mutants expressed as fusions with GAL4bd and summary of the results of plate growth and 3AT inhibition assays. Numbers of the first and last amino acids of each construct are shown. The results of plate assays for growth in the absence of histidine (performed as shown in Fig. 2*A*) are indicated by the + or − signs. The results of 3AT inhibition assays are indicated as the concentration of 3AT that causes 50% inhibition of growth in −His medium (IC_{50}). *B*, β-galactosidase assays. Expression of the *lacZ* reporter gene in yeast cells transformed with GAL4ad-β2 and GAL4bd-μ2 deletion mutants was quantified using a chemiluminescent β-galactosidase assay. Results are the mean ± standard deviation of triplicate determinations expressed in relative light units (*RLU*).

sion of β-galactosidase activity (Fig. 1).

A qualitative assay for growth on −His plates confirmed that both μ1 and μ2 interacted with β2 and with the YQRL signal (Fig. 2*A*). Interactions with the signal were dependent upon the critical tyrosine residue (Fig. 2*A*). To compare the apparent avidities of these interactions, we first monitored the growth of the transformed yeast strains in −His liquid medium (Fig. 2*B*). In this assay, stronger interactions result in higher rates of growth. In addition, we developed a more discriminating assay in which the growth of transformed yeast strains in −His liquid medium was measured in the presence of varying concentrations of 3AT, an inhibitor of the *HIS3*-encoded enzyme imidazole-glycerol-phosphate dehydratase (Fig. 2*C*). In this assay, the stronger the interactions between the two-hybrid partners, the higher the concentration of 3AT needed to inhibit growth. Both quantitative growth assays indicated that μ2-β2 interactions were somewhat stronger than μ1-β2 interactions (Fig. 2, *B* and *C*), consistent with previously published data (4). The assays also revealed that μ2-YQRL interactions were much stronger than μ1-YQRL interactions, as evidenced by the marked differences of growth in liquid medium (Fig. 2*B*) and by the shift (2 orders of magnitude) of the 3AT inhibition curves (Fig. 2*C*).

Delineation of Regions of μ2 Involved in Interactions with β2 and with the YQRL Signal—To delineate the region of μ2 involved in interactions with β2, we constructed a series of μ2 deletion mutants (Fig. 3*A*) and evaluated them by two-hybrid assays for growth on −His plates (Fig. 3*A*), resistance to growth inhibition by 3AT (Fig. 3*A*), and β-galactosidase activity (Fig. 3*B*). All assays gave similar results. Deletion of the amino-terminal 120 amino acids of μ2 (construct 121–435) abrogated interaction with β2. In contrast, constructs with deletions of up

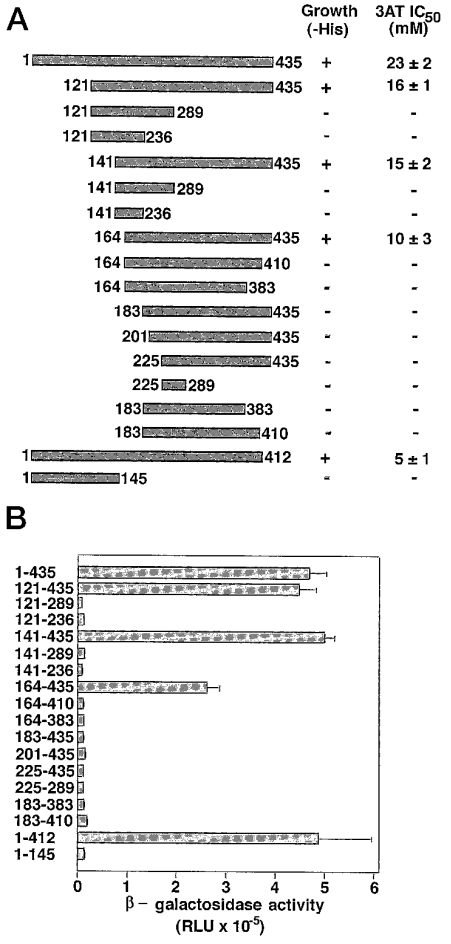

FIG. 4. **Analysis of the interaction of the YQRL signal with μ2 deletion mutants.** Interactions were analyzed by transformation of yeast cells with plasmids encoding GAL4bd-YQRL and GAL4ad-μ2 deletion mutants (as shown in Fig. 1*B*). *A*, diagram of μ2 deletion mutants expressed as fusions with GAL4ad and summary of the results of plate growth and 3AT inhibition assays. *B*, β-galactosidase assays. For more details on assays, see legend to Fig. 3.

to 290 amino acids from the carboxyl terminus of μ2 (*e.g.* construct 1–145) were able to interact with β2. A further deletion leaving the amino-terminal 70 amino acids of μ2 (construct 1–70), however, completely abolished interaction with β2. These observations suggested that the binding site for β2 is contained within an amino-terminal segment of μ2 comprising amino acids 1–145.

The same assays were used to examine interaction of μ2 deletion mutants with the YQRL signal (Fig. 4, *A* and *B*). We found that deletion of up to 163 amino acids from the amino terminus of μ2 (*e.g.* construct 164–435) had little or no effect on the ability of the protein to bind YQRL. Deletion of an additional 19 amino acids (construct 183–435), however, prevented interaction with the signal. Truncation of the last 23 amino acids from the carboxyl terminus of μ2 (construct 1–412) did not prevent interaction with the signal, but removal of 25 amino acids from the carboxyl terminus of a construct starting at amino acid 164 (construct 164–410) led to a complete loss of interaction. From these observations, we concluded that the Y*XX*Ø-binding region is contained within a carboxyl-terminal segment spanning amino acids 164–435, with the suggestion that the last 23 amino acids are dispensable for interactions.

Taken together, the above experiments indicate that the ability to interact with β2 resides within the amino-terminal one-third of μ2, whereas interactions with Y*XX*Ø-type signals are a function of the carboxyl-terminal two-thirds of the protein

TABLE I
Binding characteristics of μ2 point mutants analyzed by 3AT inhibition assays

All residues targeted for mutagenesis were identical in μ2 and μ1, except for Ile-96 in μ2, which is replaced by a leucine in μ1. The β2 and YQRL binding activity of the different mutants was estimated by determining the ratio of half-maximal inhibitory concentrations of 3AT according to the formula: $(IC_{50})_{mutant}/(IC_{50})_{WT}$. The $(IC_{50})_{WT}$ values for μ2 binding to β2 and YQRL were 34 ± 2 mM and 23 ± 2 mM, respectively. The results are expressed as the mean ± standard deviation of three determinations.

Mutants	$(IC_{50})_{mutant}/(IC_{50})_{WT}$	
	β2 binding	YQRL binding
L82A	0.30 ± 0.05	0.78 ± 0.20
Y83A	0.58 ± 0.15	0.80 ± 0.14
I96A	0.11 ± 0.03	0.74 ± 0.18
E98A	0.70 ± 0.20	0.80 ± 0.10
D176A	1.03 ± 0.10	0.60 ± 0.10
M209A	0.98 ± 0.12	0.02 ± 0.01
F265A	0.96 ± 0.15	0.20 ± 0.07
D269A	0.95 ± 0.10	0.20 ± 0.12
G270A	1.10 ± 0.20	0.20 ± 0.06

(see scheme in Fig. 8).

Effects of Single Amino Acid Substitutions on Interactions of μ2 with β2 and the YQRL Signal—To further define the regions of μ2 involved in interactions with β2 and with the YQRL signal, we introduced single amino acid substitutions (to alanine) within segments of μ2 that are highly homologous to segments of μ1 (Table I; see Fig. 8 for position of the residues). Most of the amino acids targeted for mutagenesis were identical in μ2 and μ1 and were contained within either the β2-binding region (Leu-82, Tyr-83, Ile-96, and Glu-98) or the Y*XX*Ø-binding region of μ2 (Asp-176, Met-209, Phe-265, Asp-269, and Gly-270). We expected that the conservation of these amino acids would reflect an essential requirement for structure or function. The mutated μ2 constructs were tested for interactions using the 3AT growth inhibition assay (Table I) and the β-galactosidase assay. The results of both assays demonstrated that mutation of Leu-82, Tyr-83, or Ile-96 significantly decreased interaction with β2 but had little or no effect on the interaction with the YQRL signal (Table I and Fig. 5, *A* and *B*). Conversely, mutation of either Asp-176, Met-209, Phe-265, Asp-269, or Gly-270 had no effect on interaction with β2 but significantly decreased interaction with the YQRL signal (Fig. 5, *A* and *B*). Mutation of Glu-98 resulted in slight but significant decreases in interactions with both β2 and YQRL, suggesting that this particular mutation has a more general effect on the structure of μ2. The differential effects of most of these mutations are consistent with the results of the deletion analysis (Figs. 3 and 4) and thus reaffirm the idea that the β2- and Y*XX*Ø-binding sites are contained within the segments 1–145 and 164–435, respectively. The fact that various mutations resulted in reduction of binding suggests that the conserved residues tested are either all involved in interactions with β2 or Y*XX*Ø or required for the conformational integrity of the β2- and Y*XX*Ø-binding domains.

Mapping of the Regions of μ1 Involved in Interactions with β2 and with the YQRL Signal—As shown in Fig. 2, μ1 is also capable of interacting with β2 and Y*XX*Ø-type signals (4, 10–12). This observation, in conjunction with the fact that μ1 and μ2 share 40% identity and 64% similarity over the entire length of their polypeptide chains (32), suggests that μ1 and μ2 may have a similar domain organization. To test this hypothesis, we constructed a small number of μ1 deletion mutants (Fig. 6) that were analogous to key μ2 constructs. Using various yeast two-hybrid assays, we found that segments of μ1 spanning amino acids 1–145 and 147–423 interacted with β2

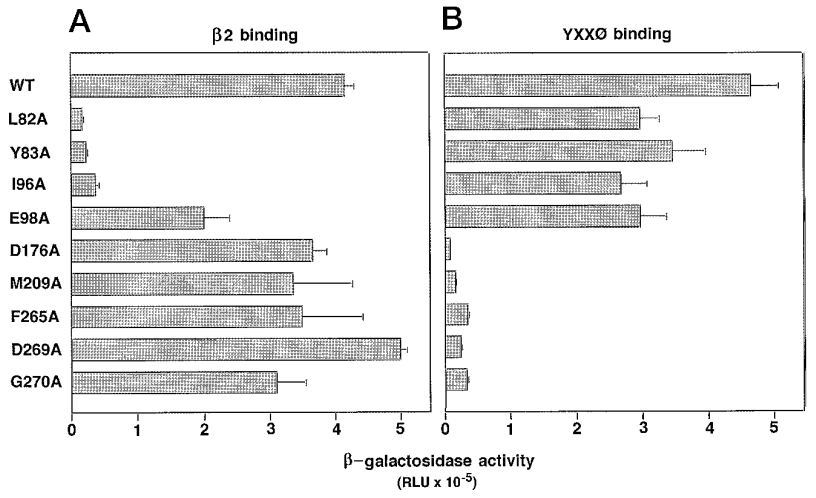

FIG. 5. **Analysis of the interaction of μ2 point mutants with β2 and the YQRL signal.** Mutants of μ2 carrying single amino acid substitutions to alanine were examined for interaction with β2 (*A*) and YQRL (*B*) by the two-hybrid analyses described in the legend to Fig. 1. The figure shows the results of β-galactosidase assays, which are expressed as the mean ± standard deviation of triplicate determinations in relative light units (*RLU*). *WT*, wild type.

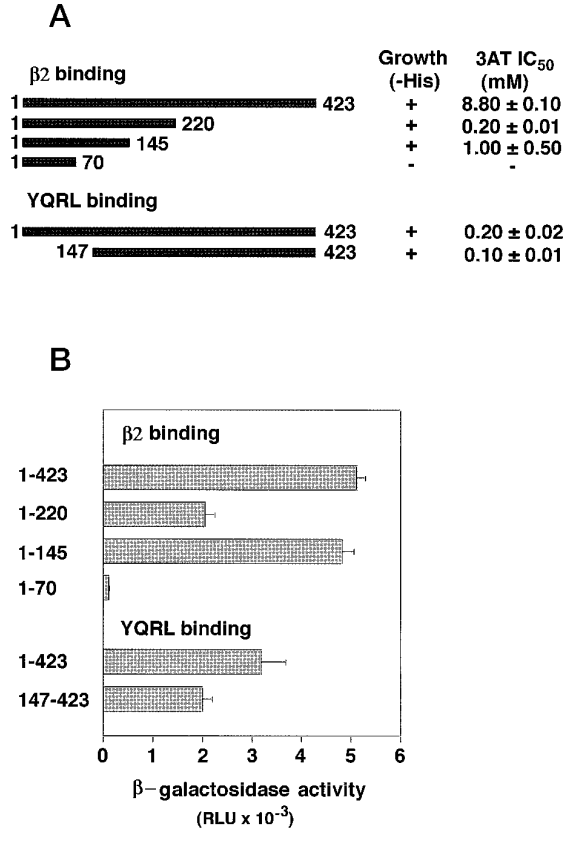

FIG. 6. **Analysis of the interaction of μ1 deletion mutants with β2 and the YQRL signal.** The μ1 deletion mutants shown in *A* were tested for interactions with β2 and with the YQRL signal by two-hybrid analyses similar to those described in the legend to Fig. 1. *A*, diagram of the μ1 deletion mutants and summary of the results of plate growth and 3AT inhibition assays. *B*, β-galactosidase assays. For more details on assays, see legend to Fig. 3.

and YQRL, respectively (Fig. 6). This observation indicated that μ1 and μ2 have a similar, bipartite domain organization.

Domain Mapping of μ2 by Proteolytic Digestion of the AP-2 Complex—All the experiments described thus far were performed with isolated medium chains using the yeast two-hybrid system. To examine how these results correlated with the domain organization of μ2 in the context of the complete AP-2 complex, we performed proteolytic digestion experiments. To this end, we treated purified brain clathrin-coated vesicles (CCVs), which contain clathrin-AP-2 assemblies, with trypsin. Digestions were performed on CCVs rather than purified AP-2 because μ2 was found to be more sensitive to proteolysis in CCVs (33). The trypsin-digested samples were analyzed by SDS-PAGE and immunoblotting using antibodies to AP-2 subunits (Fig. 7). As expected from previous work (6, 16–18), the α and β chains were cleaved into ~60-kDa and ~40-kDa fragments, which corresponded to the head and ear domains, respectively (Fig. 7, *A–D*).

The cleavage pattern of μ2 was investigated using an antibody to residues 11–29 of the protein (Fig. 7*F*); thus, all the μ2 fragments identified in the immunoblots contained the amino terminus of the protein. Treatment with low concentrations of trypsin resulted in cleavage of full-length μ2 (apparent molecular mass ~50 kDa) into a species of 27 kDa; with increasing trypsin concentrations, the 27-kDa species disappeared concomitant with the appearance of a 25-kDa species (Fig. 7*F*). These observations are in agreement with previous work of Matsui and Kirchhausen (33), who demonstrated that a similarly generated 25-kDa fragment of μ2 corresponds approximately to the amino-terminal half of the protein. Treatment with higher concentrations of trypsin resulted in conversion of the 27–25-kDa species into a 17-kDa fragment and eventually a 15-kDa fragment (Fig. 7*F*). No fragments smaller than 15 kDa were observed, even at the highest concentration of trypsin tested (1.25 mg/ml); at this concentration, virtually all of the μ2 was cleaved into the 15-kDa fragment (Fig. 7*F*). Thus, these experiments demonstrated the existence of trypsin-sensitive sites at about one-third and one-half of the μ2 polypeptide chain, from the amino terminus. The amino-terminal one-third of μ2 likely represents an independent folding domain of μ2 and roughly corresponds to the region of μ2 involved in β2 binding. The resistance of this μ2 domain to proteolysis may be due to its location within the AP-2 core. On the other hand, the carboxyl-terminal two-thirds of μ2 (which contains the Y*XX*Ø-binding region) appear to be accessible to the protease in the context of the AP-2 complex.

DISCUSSION

The results of the two-hybrid analyses presented here suggest that the μ2 chain of AP-2 has a bipartite structure, with the amino-terminal one-third of the molecule (amino acids 1–145) being involved in assembly with the β2 chain and the carboxyl-terminal two-thirds (amino acids 164–435) being responsible for the recognition of Y*XX*Ø-type sorting signals (Fig. 8). A more limited analysis of μ1 suggests that this protein has a similar bipartite structure. The two functional regions of μ2 are completely separable and remain fully active in the absence of the other part of the molecule. Moreover, point mutations can be introduced within each of the two regions that impair

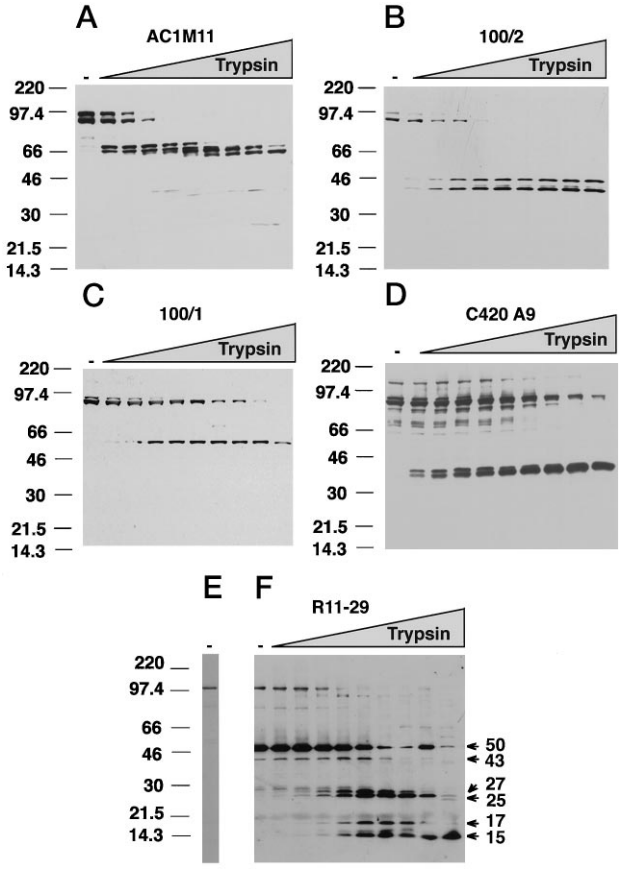

FIG. 7. **Immunoblotting of trypsin-digested AP-2 complexes with different antibodies.** CCVs were incubated in the absence (−) or presence of different concentrations of trypsin (1, 2, 4, 8, 25, 63, 125, 250, and 1250 μg/ml) and separated by SDS-PAGE. Proteins were transferred onto nitrocellulose, and blots were incubated with primary antibodies to the α, β, or μ2 subunits of AP-2 and secondary antibodies conjugated to horseradish peroxidase. Bands were detected by enhanced chemiluminescence. The primary antibodies used were: two anti-α-adaptin mouse monoclonal antibodies, AC1M11 (*A*) and 100/2 (*B*), and two anti-β-adaptin mouse monoclonal antibodies, 100/1 (*C*), C420-A9 (*D*), or R11–29 (*E* and *F*, a rabbit antibody to the amino terminus of μ2). The antibodies to α recognize two protein isoforms, α_a and α_c, both of which are components of the AP-2 complex (43). The anti-β antibodies recognize both β1- and β2-adaptins, which are components of AP-1 and AP-2, respectively. Blots probed with R11–29 were incubated in the presence or absence of 300 μg/ml competing immunogenic peptide (*E* and *F*, respectively). The positions of μ2 cleavage products and their estimated molecular masses (in kDa) are indicated by *arrows* at the *right* of *panel F*. The positions of molecular mass markers (in kDa) are indicated at the *left*.

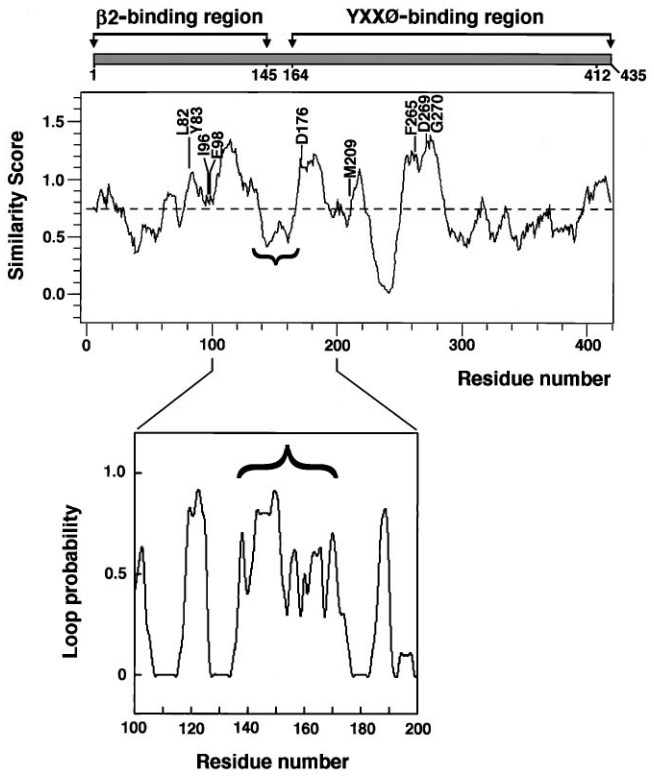

FIG. 8. **Structural features of μ2.** The *upper part* of the figure shows a schematic representation of μ2 indicating the β2-binding region (residues 1–145) and the Y*XX*Ø-binding region (residues 164–435) inferred from our experiments. A similarity plot of adaptor medium chain (μ1, μ2, μ3A, and μ3B) sequences was generated with the PLOTSIMILARITY program using a 10-amino acid window; the resulting similarity score was plotted against the residue number (average similarity score is shown as a *dotted line*). Amino acids that were mutated to alanine are also indicated. The *bracket* indicates a region of low similarity between the medium chains that exhibits a high loop probability (shown below in expanded scale), as calculated by the neural network prediction system PHD.

one type of interaction without affecting the other. The functional domain organization of μ2 suggested by the two-hybrid analyses is consistent with the location of a major trypsin-sensitive site at about one-third of the polypeptide chain relative to the amino terminus (Fig. 7). The amino-terminal one-third of the molecule is very resistant to proteolysis, which may be due to its interaction with β2 within the AP-2 core.

The β2- and Y*XX*Ø-binding domains are separated by an intervening region (at a minimum comprising amino acids 146–163) that does not appear to be required for either interaction. Comparison of adaptor medium chain sequences reveals that the 146–163 segment corresponds to a stretch of low similarity (Fig. 8, *bracket* in *upper graph*). These observations suggest that the segment encompassing amino acids 146–163 may act as a linker between the β2- and Y*XX*Ø-binding domains of μ2. Linker sequences often appear as loops in the three-dimensional structure of proteins (34). This may also be the case for the 146–163 segment, as analysis of secondary structure predicts a high probability of a loop in that region (Fig. 8, *bracket* in *lower graph*).

Another region of low sequence similarity in the adaptor medium chains occurs at amino acids 220–250 of μ2 (Fig. 8, *upper graph*). This region also contains a trypsin-sensitive site that was reported previously by Matsui and Kirchhausen (33) and confirmed in this study (Fig. 7). We speculate that this region might constitute another linker connecting two subdomains, both of which are required for Y*XX*Ø binding. The inability to trim further the Y*XX*Ø-binding region (residues 164–412) without losing binding activity may be due to the involvement of both of these subdomains in interactions with signals.

The μ1 and μ2 chains are members of a growing family of homologous coat proteins that also includes μ3A and μ3B (formerly known as p47A and p47B; Ref. 35), δ-COP (36–38), and ARP-2 (39). μ3A and μ3B are components of the recently described AP-3 complex (21, 23, 40, 41) and share ~30% identity with μ1 and μ2 (35). Like μ1 and μ2, μ3A and μ3B bind Y*XX*Ø-type signals (11, 40). Also by analogy to μ1 and μ2, we expect that μ3A and μ3B will interact with the β3A (21, 23) and β3B (β-NAP; Ref. 24) chains of AP-3, both of which are homologous to β1 and β2. δ-COP is a component of the COPI coat (38) and exhibits ~20% identity to μ1 and μ2. It is currently unknown whether δ-COP interacts with any signals; however, two-hybrid analyses have shown that it interacts with β-COP, the chain of COPI related to β1 and β2 (38). While still fragmentary, all of this evidence suggests that the μ and β chain

homologs of various coat protein complexes might be involved in similar types of interaction. Given that the homology among μ chain family members extends throughout their entire polypeptide chains, we anticipate that they will have a similar functional domain organization as well as a similar arrangement within their respective complexes.

The mode of assembly exemplified by μ-β interactions may in fact apply to other interactions within the adaptor complexes. Indeed, the small chains σ1 and σ2 have been shown to interact specifically with the γ and α chains of AP-1 and AP-2, respectively (4). Strikingly, all members of the small chain family described to date (σ1, σ2, σ3A, σ3B, and ζ-COP) bear low but significant homology to the amino-terminal half of the medium chains (37, 40, 42). This suggests that a large portion of the small chains may be dedicated to interactions with a member of the α-γ-δ family, perhaps leaving a short carboxyl-terminal extension available for some other function.

On the basis of the results presented here, we propose that the μ2 chain is anchored to the AP-2 core via interaction of β2 with an amino-terminal segment comprising approximately one-third of the μ2 polypeptide chain. The remaining two-thirds of μ2 likely project outward from the AP-2 core, placing this domain of μ2 in a position to interact with tyrosine-based sorting signals. Our data also suggest that μ1 may be similarly arranged within the AP-1 complex, and that this structural organization of the medium chains may be a general feature of all adaptor complexes.

Acknowledgments—We thank Marie-Christine Fournier for excellent technical assistance; Evan Eisenberg, Lois Green, Tomas Kirchhausen, and Margaret S. Robinson for kind gifts of reagents; and Chean Eng Ooi and Esteban Dell'Angelica for critical review of the manuscript.

REFERENCES

1. Robinson, M. (1992) *Trends Cell Biol.* **2,** 293–297
2. Kirchhausen, T. (1993) *Curr. Opin. Struct. Biol.* **3,** 182–188
3. Robinson, M. S. (1993) *J. Cell Biol.* **123,** 67–77
4. Page, L. J., and Robinson, M. S. (1995) *J. Cell Biol.* **131,** 619–630
5. Ahle, S., and Ungewickell, E. (1989) *J. Biol. Chem.* **264,** 20089–20093
6. Schröder, S., and Ungewickell, E. (1991) *J. Biol. Chem.* **266,** 7910–7918
7. Gallusser, A., and Kirchhausen, T. (1993) *EMBO J.* **12,** 5237–5244
8. Shih, W., Gallusser, A., and Kirchhausen, T. (1995) *J. Biol. Chem.* **270,** 31083–31090
9. Goodman, O. B., Jr., and Keen, J. H. (1995) *J. Biol. Chem.* **270,** 23768–23773
10. Ohno, H., Stewart, J., Fournier, M. C., Bosshart, H., Rhee, I., Miyatake, S., Saito, T., Gallusser, A., Kirchhausen, T., and Bonifacino, J. S. (1995) *Science* **269,** 1872–1875
11. Ohno, H., Fournier, M. C., Poy, G., and Bonifacino, J. S. (1996) *J. Biol. Chem.* **271,** 29009–29015
12. Boll, W., Ohno, H., Songyang, Z., Rapoport, I., Cantley, L. C., Bonifacino, J. S., and Kirchhausen, T. (1996) *EMBO J.* **15,** 5789–5795
13. Shiratori, T., Miyatake, S., Ohno, H., Nakaseko, C., Isono, K., Bonifacino, J. S., and Saito, T. (1997) *Immunity* **6,** 583–589
14. Rapoport, I., Miyazaki, M., Boll, W., Duckworth, B., Cantley, L. C., Shoelson, S., and Kirchhausen, T. (1997) *EMBO J.* **16,** 2240–2250
15. Heuser, J. E., and Keen, J. (1988) *J. Cell Biol.* **107,** 877–886
16. Zaremba, S., and Keen, J. H. (1985) *J. Cell. Biochem.* **28,** 47–58
17. Keen, J. H., and Beck, K. A. (1989) *Biochem. Biophys. Res. Commun.* **158,** 17–23
18. Kirchhausen, T., Nathanson, K. L., Matsui, W., Vaisberg, A., Chow, E. P., Burne, C., Keen, J. H., and Davis, A. E. (1989) *Proc. Natl. Acad. Sci. U. S. A.* **86,** 2612–2616
19. Robinson, M. S. (1990) *J. Cell Biol.* **111,** 2319–2326
20. Ooi, C. E., Moreira, J. E., Dell'Angelica, E. C., Poy, G., Wassarman, D. A., and Bonifacino, J. S. (1997) *EMBO J.* **16,** 4508–4518
21. Simpson, F., Peden, A. A., Christopoulou, L., and Robinson, M. S. (1997) *J. Cell Biol.* **137,** 835–845
22. Peyrard, M., Fransson, I., Xie, Y. G., Han, F. Y., Ruttledge, M. H., Swahn, S., Collins, J. E., Dunham, I., Collins, V. P., and Dumanski, J. P. (1994) *Hum. Mol. Genet.* **3,** 1393–1399
23. Dell'Angelica, E. C., Ooi, C. E., and Bonifacino, J. S. (1997) *J. Biol. Chem.* **272,** 15078–15084
24. Newman, L. S., McKeever, M. O., Okano, H. J., and Darnell, R. B. (1995) *Cell* **82,** 773–783
25. Ponnambalam, S., Robinson, M. S., Jackson, A. P., Peiperl, L., and Parham, P. (1990) *J. Biol. Chem.* **265,** 4814–4820
26. Robinson, M. S. (1987) *J. Cell Biol.* **104,** 887–895
27. Ahle, S., Mann, A., Eichelsbacher, U., and Ungewickell, E. (1988) *EMBO J.* **7,** 919–929
28. Rost, B., and Sander, C. (1993) *J. Mol. Biol.* **232,** 584–599
29. Rost, B., Sander, C., and Schneider, R. (1994) *CABIOS* **10,** 53–60
30. Rost, B., and Sander, C. (1994) *Proteins* **19,** 55–72
31. Fields, S., and Song, O. (1989) *Nature* **340,** 245–246
32. Nakayama, Y., Goebl, M., O'Brine Greco, B., Lemmon, S., Pingchang Chow, E., and Kirchhausen, T. (1991) *Eur. J. Biochem.* **202,** 569–574
33. Matsui, W., and Kirchhausen, T. (1990) *Biochemistry* **29,** 10791–10798
34. Branden, C., and Tooze, J. (1991) *Introduction to Protein Structure*, Garland Publishers, New York
35. Pevsner, J., Volknandt, W., Wong, B. R., and Scheller, R. H. (1994) *Gene (Amst.)* **146,** 279–283
36. Radice, P., Pensotti, V., Jones, C., Perry, H., Pierotti, M. A., and Tunnacliffe, A. (1995) *Genomics* **26,** 101–106
37. Cosson, P., Demolliere, C., Henecke, S., Duden, R., and Letourneur, F. (1996) *EMBO J.* **15,** 1792–1798
38. Faulstich, D., Auerbach, S., Orci, L., Ravazzola, M., Wegchingel, S., Lottspeich, F., Stenbeck, G., Harter, C., Wieland, F. T., and Tschochner, H. (1996) *J. Cell Biol.* **135,** 53–61
39. Wang, X., and Kiliman, M. W. (1997) *FEBS Lett.* **402,** 57–61
40. Dell'Angelica, E. C., Ohno, H., Ooi, C. E., Rabinovich, E., Roche, K. W., and Bonifacino, J. S. (1997) *EMBO J.* **16,** 917–928
41. Simpson, F., Bright, N. A., West, M. A., Newman, L. S., Darnell, R. B., and Robinson, M. S. (1996) *J. Cell Biol.* **133,** 749–760
42. Traub, L. M. (1997) *Trends Cell Biol.* **7,** 43–46
43. Robinson, M. S. (1989) *J. Cell Biol.* **108,** 833–842